

# perm2vec: Graph Permutation Selection for Decoding of Error Correction Codes using Self-Attention

Nir Raviv<sup>\*§</sup>, Avi Caciularu<sup>†§</sup>, Tomer Raviv<sup>\*</sup>, Jacob Goldberger<sup>‡</sup>, and Yair Be'ery<sup>\*</sup>

<sup>\*</sup>School of Electrical Engineering, Tel-Aviv University, Tel-Aviv, Israel.

<sup>†</sup>Department of Computer Science, Bar-Ilan University, Ramat-Gan, Israel.

<sup>‡</sup>Faculty of Engineering, Bar-Ilan University, Ramat-Gan, Israel.

**Abstract**—Error correction codes are integral part of communication applications, boosting the reliability of transmission. The optimal decoding of transmitted codewords is the maximum likelihood rule, which is NP-hard due to the *curse of dimensionality*. For practical realizations, suboptimal decoding algorithms are employed; yet limited theoretical insights prevents one from exploiting the full potential of these algorithms. One such insight is the choice of permutation in *permutation decoding*. We present a data-driven framework for permutation selection, combining domain knowledge with machine learning concepts such as node embedding and self-attention. Significant and consistent improvements in the bit error rate are introduced for all simulated codes, over the baseline decoders. To the best of the authors' knowledge, this work is the first to leverage the benefits of the neural Transformer networks in physical layer communication systems.

## I. INTRODUCTION

The renowned channel coding theorem of Shannon [1] states that for every channel a code exists, such that encoded messages can be transmitted and decoded with an error as low as one desires while transmission rate is below the channel's capacity. For practical applications, latency and computational complexity constrain the code's size due to the *curse of dimensionality*. Thus, *structured codes* with low complexity encoding and decoding schemes, had to be devised.

Some of the mentioned structured codes possess a main feature known as the *permutation group* (PG). The permutations in PG are ones which map every codeword to some distinct codeword. This fact is important to different decoders, such as the parallelizable soft-decision Belief Propagation (BP) [2] decoder. It empirically stems from evidence, that while decoding of various corrupted words may fail, decoding a permuted version of the same corrupted words may succeed [3]. For instance, this is exploited in the mRRD [4] and the BPL [5], which perform multiple runs over different permuted versions of the same corrupted codewords, trading-off complexity for higher decoding gains.

Nonetheless, room for improvement exists as not all permutations are required for successful decoding of a given word - a mere fitting one is needed. Our work is concerned with

obtaining the most fitting permutation per word, removing redundant runs hence preserving computational resources. Yet, how can one obtain such a permutation remains vague, as the authors of [5] indicate in their Section III.A, "*there exists no clear evidence on which graph permutation performs best for a given input*". Explicitly, one would like to approximate a function mapping from a single word to the most probable-to-decode permutation. While analytical derivation of this function is hard, advancements in the machine learning field may be of aid in the computation of such a function.

With the recent emergence of Deep Learning (DL), the success of Neural Networks (NN) is demonstrated in a myriad of communication and information theory applications where no analytical solutions exist [6], [7]. For instance in [8], a tight lower bound on the mutual information between two high-dimensional continuous variables is estimated with NN. Another recurring motive for the use of NN in communications is concerned with the amount of data that one possesses. Several data-driven solutions are offered in [9]–[11] to scenarios having small quantity of data, as obtaining data-samples in the real-world is costly and hard to collect in an on-the-fly manner. On the other hand, one should not belittle the benefits of unlimited simulated data, see [12], [13].

Lately, two main classes of decoders are considered in machine learning for decoding. The first is the class of *model-free* decoders, employing state-of-the-art (SOTA) architectures as in [14], [15]. The second is composed of *model-based* decoders [16]–[19], implementing parameterized versions of classical BP decoders. Nowadays, the model-based approach dominates, yet suffers from regularized hypothesis space due to its *inductive bias*.

Our work leverages on permutation groups and DL to enhance the decoding capabilities of the constrained model-based decoders. At first, the Transformer encoder (introduced in Section II-D) [20] is employed to embed all distinguished group permutations of a code in a word independent manner, extracting relevant features. This is done *once* in advance to the test phase during a preprocess phase. At test time, a trained NN accepts a corrupted word and the embedded permutations and predicts for each permutation the probability for successful decoding. Thereafter, a set of either one, five or ten most-probable to decode permutations are chosen, and decoding is carried out on the permuted channel-words. That is, instead

Correspondence to: Nir Raviv (nirraviv89@gmail.com), Avi Caciularu (avi.c33@gmail.com)

<sup>§</sup>Equal contribution

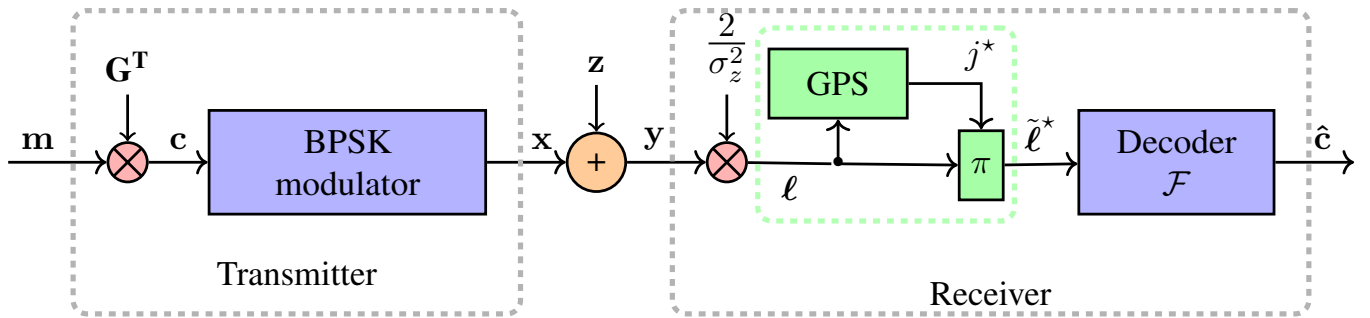


Fig. 1: Diagram of a communication system. Our proposed Graph Permutation Selection (GPS) block and the permutation function  $\pi$  are colored in green.

of decoding an arbitrary dataset with all permutations, and empirically choosing the best subset of them.

The remainder of this paper is organized as follows. The background on coding, code permutations, node embedding and self-attention is provided in Section II. The formulation and method of the Graph Permutation Selection (GPS) is presented in Section III. The experimental setup and results are detailed in Section IV. Finally, Section V and Section VI discusses related works and concludes this paper, respectively.

## II. BACKGROUND

### A. Coding

A typical communication system is depicted in Fig. 1 (excluding the green dashed-block). First, a length  $k$  binary message  $\mathbf{m} \in \{0, 1\}^k$ , such that  $\mathbf{m}$  is a column vector (and all following vectors are assumed to be the same), is encoded to form a length  $n$  codeword  $\mathbf{c} \in \{0, 1\}^n$ . That is, according to a chosen code  $\mathbb{C}$  with a generator matrix  $\mathbf{G}$  by  $\mathbf{c} = \mathbf{G}^T \mathbf{m}$ . Generally, every codeword  $\mathbf{c}$  satisfies  $\mathbf{H}\mathbf{c} = \mathbf{0}$ ,  $\mathbf{H}$  being the parity-check matrix (uniquely defined by  $\mathbf{G}\mathbf{H}^T = \mathbf{0}$ ). Next, the codeword  $\mathbf{c}$  is modulated by the Binary Phase Shift Keying (BPSK) mapping ( $0 \rightarrow 1, 1 \rightarrow -1$ ) resulting in a modulated word  $\mathbf{x}$ . After transmission through the additive white Gaussian noise (AWGN) channel, the received word is  $\mathbf{y} = \mathbf{x} + \mathbf{z}$ , where  $\mathbf{z} \sim N(\mathbf{0}, \sigma_z^2 \mathbf{I}_n)$ . Usually, it is more convenient to consider the log likelihood ratio (LLR) for either validating the received word is error-free or for soft-decoding. The LLR values in the AWGN case are given by  $\ell = \frac{2}{\sigma_z^2} \cdot \mathbf{y}$ , and knowledge of  $\sigma_z$  is assumed.

At the receiver, one initially checks whether the received word contains any detectable errors. For that purpose, the syndrome  $\mathbf{s} = \mathbf{H}\hat{\mathbf{c}}$  is compared to the zeros vector (the comparison is known as the *syndrome stopping criterion*). Estimated codeword  $\hat{\mathbf{c}}$  is calculated following the hard decision (HD) rule:

$$\hat{c}_i = \begin{cases} 1, & \text{if } \ell_i < 0 \\ 0, & \text{otherwise.} \end{cases}$$

If the syndrome is all-zeros, one outputs  $\hat{\mathbf{c}}$  and concludes. On the other hand, non-zero syndrome indicates that channel errors occurred. Then, one utilizes a decoding function  $\mathcal{F} : \mathbb{R}^n \rightarrow \{0, 1\}^n$ , with output  $\hat{\mathbf{c}} = \mathcal{F}(\ell)$ . One such soft-decision

decoding algorithm is the Belief Propagation (BP) described ahead.

The BP is a graph-based inference algorithm used to decode corrupted codewords in an iterative manner, working over a graphical structure known as the *Tanner graph*. The Tanner graph is an undirected bipartite graph, constructed of nodes and edges. The nodes in the Tanner graph are of two types - variables and checks nodes. An edge exists between a variable node  $n$  and a check node  $h$  iff variable  $n$  participates in the condition defined by the  $h^{\text{th}}$  row in the parity-check matrix  $\mathbf{H}$  of code  $\mathbb{C}$ . The BP operates by passing messages over the nodes of the Tanner graph until convergence or a maximum number of iterations is reached. One property known to effect the convergence of the algorithm are *cycles*. Cycles in a Tanner graph refer to a subset of nodes connected to each other and inducing a closed loop with every edge appearing once. Message propagated along these cycles become correlated after several BP iterations, preventing convergence; thus reducing overall decoding performance. We refer the interested reader to [21] for a full derivation of the BP for linear codes, and to [22] for more details on the effects of cycles in codes.

Previous works [16], [18] assigned learnable weights  $\theta$  to the BP algorithm (a model-based approach mentioned in Section I). This formulation unfolds the BP algorithm into a NN, referred to as weighted BP (WBP). The intuition offered was that the trained weights compensate for the short cycles (these are most performance devastating) in the Tanner graph.

### B. Permutations

One possible way to mitigate the detrimental effects of cycles is by using code *permutations*. Permuting the LLRs leads to a different initialization of the BP algorithm messages. This is proved to yield to a better convergence and overall decoding performance gain [4], and can be further observed in our experiments, in Section IV. The permutation of a codeword is a function  $\pi : i \rightarrow \pi(i)$  exchanging positions of bits in a codeword  $\mathbf{c}$  (or in a LLR word  $\ell$ ):

$$\mathbf{c}^{(\pi)} = (c_{\pi(0)}, c_{\pi(1)}, \dots, c_{\pi(n-1)})^T.$$

A permutation  $\pi$  is an *automorphism* if for all codewords, their permuted version is also a codeword, that is  $\mathbf{c}^{(\pi)} \in \mathbb{C}, \forall \mathbf{c} \in \mathbb{C}$ . The group of all automorphism permutations of a code  $\mathbb{C}$  is denoted  $\text{Aut}(\mathbb{C})$ , also referred to as the PG of the code.

Only several codes have known PGs [23] such as the BoseChaudhuriHocquenghem (BCH) codes, given in [24] [pp.233] as:

$$\pi_{\alpha,\beta}(i) = [2^\alpha \cdot i + \beta] \pmod{n}$$

with  $\alpha \in \{1, \dots, \log_2(n+1)\}$  and  $\beta \in \{1, \dots, n\}$ . Thus a total of  $n \log_2(n+1)$  permutations compose  $Aut(\mathbb{C})$ .

### C. Node Embedding

The method we propose uses *node embedding* technique for incorporating the code information by taking the code’s Tanner graph into consideration, which is detailed in Sec. III-B. Specifically, we choose to employ the *node2vec* [25] method. We shortly describe this method and the reader can further refer to the paper for more technical details.

The task of *node embedding* aims to encode nodes in a graph as low-dimensional vectors that summarize their relative graph position and the structure of their local neighborhood. Each learned vector corresponds to a node in the graph, and it was shown that in the learned vector space, geometric relations are captured, e.g., interactions that are modeled as edges between the nodes in the graph.

Specifically, *node2vec* is trained by maximizing the mean probability of the occurrence of subsequent nodes in fixed length sampled random walks. It employs both breadth-first (BFS) and depth-first (DFS) graph searches to produce high quality informative node representations.

### D. Self-Attention

Attention mechanism for neural networks was designed to help neural models focus on the most relevant parts of the input. This modern neural architecture allows using weighted averaging to optimize a task objective and to deal with variable sized inputs. When feeding an input sequence to an attention model, the resulted output is an embedded representation of the input. When a single sequence is fed, the attentive mechanism is employed to attend to all positions within the same sequence. This is commonly referred to as the *self-attention* representation of a sequence. Initially, self-attention modelling was used in conjunction with recurrent neural networks (RNNs) and convolutional neural networks (CNNs) mostly for natural language processing (NLP) tasks. In [26], this setup was employed first and was shown to produce superior results on multiple automatic machine translation tasks.

Recently, an advanced form of modelling attentive relations was introduced. Transformer networks allows modeling inter-sequence dependencies regardless to the position in the input sequence. [20] demonstrated that machine translation models could achieve SOTA results by solely using this self-attention model. A more recent family of Transformer-based self-attentive models [27]–[29], uses multiple self-attention layers, significantly advanced the SOTA in various linguistic tasks rather than machine translation, e.g. question answering [29], coreference resolution [30] and a variety of linguistic tasks according to the GLUE benchmark [31].

This self-attention mechanism allows a better and richer permutation modelling compared to a non-attentive learned

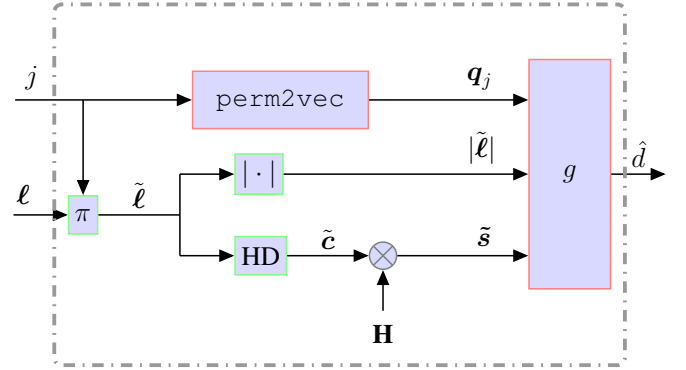


Fig. 2: Our schematic architecture - *perm2vec* and the permutation classifier.

representation. The motivation behind using self-attention comes from permutation distance metrics preservation; a pair of “similar” permutations will have a close geometric self-attentive representation in the learned vector space, since the number of indices swaps between permutations affects just the positional embeddings additions. We also experienced a major performance improvement using self-attention which is not reported in this paper. Moreover, at test time, our self-attentive representation requires just one single pass for an embedding table computation (which is stored and can be reused) so the Transformer does not contribute for the inference complexity (more details appear in Section III-D).

## III. METHOD

Recall that picking a permutation from the PG may result in better decoding capabilities. To that end, we now describe our method. Our proposed architecture outputs an estimate to the probability of successful decoding under a given permutation in PG. This is done on a per-word basis, for every permutation in the PG. At last, decoding is executed using the permutation corresponding to the highest estimated probability. The problem setup and architecture are further presented in the rest of this section.

### A. Problem Formulation

Choosing the best permutation by executing the decoding algorithm for each permutation within the PG is a computationally prohibitive task. Explicitly, one would select a single permutation  $\pi^* \in Aut(\mathbb{C})$  for every tuple  $(\ell, \mathbf{c})$ , of received LLR word  $\ell$  and the correct codeword  $\mathbf{c} \in \mathbb{C}$ , such that the bit error rate (BER) is minimized:

$$\pi^* = \arg \min_{\pi_j \in Aut(\mathbb{C})} \text{BER} \left( \mathcal{F}(\ell^{(\pi_j)}), \mathbf{c}^{(\pi_j)} \right) \quad (1)$$

and we denote  $\tilde{\ell} \triangleq \ell^{(\pi_j)}$  and  $\tilde{\mathbf{c}} \triangleq \mathbf{c}^{(\pi_j)}$ .

We recall the definition of the BER between a codeword  $\mathbf{c}$  and its estimation  $\hat{\mathbf{c}} = \mathcal{F}(\ell)$ :

$$\text{BER}(\hat{\mathbf{c}}, \mathbf{c}) \triangleq \frac{1}{n} \sum_{i=1}^n \mathbb{1}(\hat{c}_i \neq c_i) \quad (2)$$

and  $\mathbb{1}(\cdot)$  is the indicator function.

As the solution to Eq. (1) is intractable, we propose a data-driven approach as an approximate solution. We highlight key points below, and elaborate on each one in the rest of this section.

Our architecture is depicted in Fig. 2. The main components are the *permutation embedding* (Section III-B) and the *permutation classifier* (Section III-C). First, the permutation embedding block `perm2vec` receives an index  $j$ , corresponding to a permutation from PG, and outputs an embedding  $\mathbf{q}_j$ . Next, the received word  $\ell$  is permuted by  $\pi_j$  and decomposed into a magnitude part  $|\tilde{\ell}|$  and a permuted syndrome  $\tilde{\mathbf{s}}$ . The mentioned vectors enter the permutation classifier  $g$ . The classifier assigns probability  $\hat{d}(\ell, j)$  per permutation, estimating the probability of word  $\ell$  to be successfully decoded by  $\mathcal{F}$  under permutation  $j$ . At last, the index of the maximal  $\hat{d}$  is chosen by the GPS block,

$$j^* = \arg \max_{j \in \{j' | \pi_{j'} \in \text{Aut}(\mathbb{C})\}} \hat{d}(\ell, j) \quad (3)$$

and decoding is done on  $\tilde{\ell}^* \triangleq \ell^{(\pi_{j^*})}$ . After decoding, the decoded word is depermuted and  $\hat{c}$  is output. The depermutation is omitted in Fig. 1 to prevent overburdening.

Notice that in our scheme, neither is one required to know  $c$  nor run the decoder on all permutations to choose  $j^*$ ; both facts are compulsory for practical realizations.

### B. Permutation Embedding

The Transformer model employs an encoder-decoder structure, consisting of stacked encoder and decoder layers. In this work, we use the Transformer encoder architecture which is described next, and thus we omit the details regarding the decoder part. Our modified Transformer encoder consists of two sublayers: self-attention followed by an average pooling layer. To the best of our knowledge, our work is the first to leverage the benefits of the neural Transformer network in physical layer communication systems.

In [20], positional encodings are vectors that are originally compound with entries based on sinusoids of varying frequency. They are added to encoder input elements prior to the first layer, which is done in order to add a position-dependent signal to each embedded token and help the model incorporate the order of the input tokens, by injecting information about the relative or absolute position of the tokens. Inspired by this method and other recent NLP works [27]–[29], we used learned positional embeddings which proved to yield better performance than the constant positional encodings, but instead of randomly initializing them, we first pre-train *node2vec* node embeddings over the corresponding code’s Tanner graph. We then take the variable nodes output embeddings to serve as the initial positional embeddings. This helps our model to incorporate some graph structure and to use the code information. We denote by  $d_w$  the dimension of the output embedding space (this hyperparameter is set before the node embedding training). It should be noted that any other node embedding model can be trained instead of *node2vec* that we leave for future work.

Self-attention sublayers usually employ multiple attention heads, but we found that using one attention head was sufficient.

Denote the embedding vector of the  $i^{\text{th}}$  position under permutation  $\pi$  by  $\mathbf{u}_i \in \mathbb{R}^{d_w}$  and the  $i^{\text{th}}$  positional embedding by  $\mathbf{v}_i \in \mathbb{R}^{d_w}$ . Note that both  $\mathbf{u}_i$  and  $\mathbf{v}_i$  are learned, but as stated before,  $\mathbf{v}_i$  is initialized with the  $i^{\text{th}}$  output of the pre-trained variable node embedding over the code’s Tanner graph.

Thereafter, the augmented attention head operates on an input vector sequence,  $\mathbf{W} = (\mathbf{w}_1, \dots, \mathbf{w}_n)$  of  $n$  vectors where  $\mathbf{w}_i \in \mathbb{R}^{d_w}$ ,  $\mathbf{w}_i = \mathbf{u}_i + \mathbf{v}_i$ . The attention head computes a same-length vector sequence  $\mathbf{P} = (\mathbf{p}_1, \dots, \mathbf{p}_n)$ , where  $\mathbf{p}_i \in \mathbb{R}^{d_p}$ .

Each encoder’s output vector,  $\mathbf{y}_i$ , is computed as a weighted sum of linearly transformed input entries,

$$\mathbf{p}_i = \sum_{j=1}^n a_{ij} (\mathbf{V} \mathbf{w}_j)$$

each attention weight coefficient,  $a_{ij}$ , is computed using the softmax function,

$$a_{ij} = \frac{e^{b_{ij}}}{\sum_{m=1}^n e^{b_{im}}}$$

where  $b_{ij}$  is the normalized relative attention between two input vectors  $\mathbf{w}_i$  and  $\mathbf{w}_j$ ,

$$b_{ij} = \frac{(\mathbf{Q} \mathbf{w}_i)^T (\mathbf{K} \mathbf{w}_j)}{\sqrt{d_p}}$$

and  $\mathbf{Q}, \mathbf{K}, \mathbf{V} \in \mathbb{R}^{d_w \times d_p}$  are learned parameters matrices.

Finally, the self-attentive vector representation of the input sequence,  $\mathbf{q} \in \mathbb{R}^{d_p}$  is computed by applying the average pooling operation across the sequence of output vectors,

$$\mathbf{q} = \frac{1}{n} \sum_{i=1}^n \mathbf{p}_i. \quad (4)$$

and enters the permutation classifier.

### C. Permutation Classifier

We wish to construct a classifier that predicts the probability of a successful decoding given a permuted noisy word. The Transformer encoder output computed at Eq. (4) forms the input passed to a neural multilayer perceptron (MLP) together with the absolute value of the permuted input LLRs  $\ell$  and the permuted syndrome  $\tilde{\mathbf{s}} \in \mathbb{R}^{n-k}$ . The full end-to-end system is depicted in Fig. 2. We first use linear mapping to obtain  $\ell' \in \mathbb{R}^{d_p}$ ,  $\ell' = \mathbf{W}_\ell \cdot |\tilde{\ell}|$  and  $\mathbf{s}' \in \mathbb{R}^{d_p}$ ,  $\mathbf{s}' = \mathbf{W}_s \cdot \tilde{\mathbf{s}}$  respectively, where  $\mathbf{W}_\ell \in \mathbb{R}^{n \times d_p}$ ,  $\mathbf{W}_s \in \mathbb{R}^{(n-k) \times d_p}$  are learned matrices. Then, inspired by [31], we use the following similarity function:

$$g(\mathbf{h}) = \mathbf{w}_4^T \Phi_3(\Phi_2(\Phi_1(\mathbf{h}))) + \mathbf{b}_4 \quad (5)$$

where,

$$\mathbf{h} = [\mathbf{q}; \ell'; \mathbf{s}'; \mathbf{q} \circ \ell'; \mathbf{q} \circ \mathbf{s}'; \ell' \circ \mathbf{s}'; |\mathbf{q} - \ell'|; |\mathbf{q} - \mathbf{s}'|; |\ell' - \mathbf{s}'|].$$

Here  $[\cdot]$  stands for concatenation and  $\circ$  stands for the Hadamard product. We also define

$$\Phi_i(\mathbf{x}) = \text{LeakyReLU}(\mathbf{W}_i \mathbf{x} + \mathbf{b}_i)$$

TABLE I: Values of the hyper-parameters, Transformer encoder and classifier.

SYMBOL	DEFINITION	VALUE
lr	Learning rate	$10^{-3}$
-	Optimizer	Adam
$d_w$	Input embedding size	80
$d_p$	Output embedding size	80
-	<i>LeakyReLU</i> Negative slope	0.1
-	SNR range [dB]	1 – 7
$K$	Mini-batch size	5000
-	Number of mini-batches	$10^5$

where  $\mathbf{W}_1 \in \mathbb{R}^{9d_p \times 2d_p}$ ,  $\mathbf{W}_2 \in \mathbb{R}^{2d_p \times d_p}$ ,  $\mathbf{W}_3 \in \mathbb{R}^{d_p \times d_p/2}$  and  $\mathbf{W}_4 \in \mathbb{R}^{d_p/2}$  are the learned matrices and  $\mathbf{b}_1 \in \mathbb{R}^{2d_p}$ ,  $\mathbf{b}_2 \in \mathbb{R}^{d_p}$ ,  $\mathbf{b}_3 \in \mathbb{R}^{d_p/2}$  and  $\mathbf{b}_4 \in \mathbb{R}$  are the learned biases respectively.

Finally, the estimated probability for successful decoding,  $\hat{d}$ , is computed as follows,

$$\hat{d} = \sigma(g(\mathbf{h}))$$

with  $g(\mathbf{h})$  being the classifier output and  $\sigma(x) = (1 + e^{-x})^{-1}$  is the sigmoid function.

#### D. Training Details

We *jointly train* both the permutation embedding and the permutation classifier, employing a single decoder  $\mathcal{F}$ . To that end, we minimize the binary cross entropy loss<sup>1</sup>:

$$\mathcal{L} = -\frac{1}{K} \sum_{j=1}^K \left[ d_j \log(\hat{d}_j) + (1 - d_j) \log(1 - \hat{d}_j) \right]$$

where  $d_j = 1$  if decoding of  $\ell_j$  was successful under permutation  $\pi$ , otherwise  $d_j = 0$ , and  $K$  is the mini-batch size. The set of decoders  $\mathcal{F}$  used for the dataset generation is described in Section IV.

Each mini-batch consists of  $K$  sampled examples from the generated training dataset. This dataset contains pairs of permuted LLR together with a corresponding label. The LLRs are calculated from the all-zero transmitted codeword ( $\mathbf{c} = (0, \dots, 0)^T$ ) and channel realizations, and the labels were produced by passing the LLRs through the decoder. Empirically, using only the all-zero word seems to be sufficient for training. Nonetheless, the test dataset is composed of randomly chosen binary codewords  $\mathbf{c} \in \mathbb{C}$ , as one would expect, without any degradation in performance.

Each codeword is transmitted over the AWGN channel with  $\sigma_z$  specified by a given *signal-to-noise ratio* (SNR), with an equal amount of positive examples ( $d=1$ ) and negative examples ( $d=0$ ) in each batch. The overall hyperparameters used for training the Transformer encoder and the MLP classifier are depicted in Table I.

For pre-training the node embeddings, we used the default hyperparameters suggested by the original work. That is, except for the next changes: The number of random walks 2000,

walk length 10, neighborhood size 10 and node embedding dimension  $d_w = 80$ .

Observe that as `perm2vec` solely depends on a given permutation (per code), all embeddings can be computed once and stored in memory. Then at test time, determination of  $j^*$  in Fig. 1 depends on the latency of  $n \log_2(n+1)$  parallelizable forward-passes in  $g$ .

## IV. EXPERIMENTAL SETUP AND RESULTS

The proposed algorithm is evaluated on four different BCH codes - (31, 16), (63, 36), (63, 45) and (127, 64). As for the decoder  $\mathcal{F}$ , we applied our method on top of the BP (**P2V+BP**) and on top of a pre-trained WBP (**P2V+WBP**), trained with the configuration from [17]. All decoders are tested with 5 BP iterations and the syndrome stopping criterion is adopted after each iteration (as described in Section II-A). These decoders are based on the *systematic* parity-check matrices,  $\mathbf{H} = \begin{bmatrix} \mathbf{P}^T & \mathbf{I}_{n-k} \end{bmatrix}$ , as these matrices are commonly used. For comparison, we employ the random permutation selection (from the PG) as a baseline for each decoder - **BP (random)** and **WBP (random)**. In addition, we depict the **maximum likelihood** results, which are the theoretical lower bound for each code (for more details, see [21], Section 1.5).

*a) Performance Analysis:* We assess the quality of our GPS using the BER metric, as in Eq. (2), for different SNR values [dB] when at least 1000 errored words occurred. Note that we will refer as SNR the normalized SNR ( $E_b/N_0$ ), which is commonly used in digital communication.

Fig. 3 presents the results for BCH(31,16) and BCH(63,36) and Table II lists the results for all codes and decoders, with our permutation selection method or with random selection. For clarity, in Table II we present the BER negative decimal logarithm only for the practical baselines, considered as the *top-1* results.

As can be seen, using our preprocess method introduces superiority over the examined baselines. For BCH(31,16) (Fig. 3a), `perm2vec` together with BP gains up to 2.75 dB over the random BP and up to 1.8 dB over the random WBP. Similarly, for BCH(63,36) (Fig. 3b), our method outperforms the random BP by up to 2.75 dB and by up to 2.2 dB comparing WBP. We also observed a small gap between our method and the maximum likelihood lower bound. The maximal gaps are 0.4 dB and 1.4 dB for BCH(31,16) and BCH(63,36), respectively.

*b) Top- $\kappa$  Evaluation:* In order to evaluate our classifier confidence, we also experiment the performance among top- $\kappa$  permutations. This extends Eq. (3) from top-1 to the desired top- $\kappa$ . The selected codeword  $\hat{\mathbf{c}}^*$  is chosen from a list of  $\kappa$  decoders by  $\hat{\mathbf{c}}^* = \arg \max_{\kappa} \|\mathbf{y} - \hat{\mathbf{c}}_{\kappa}\|_2^2$ , as in [4].

The results for  $\kappa \in \{1, 5\}$  are depicted in Table II and Fig. 4. Generally, as  $\kappa$  increases a greater performance is observed, with the added-gain gradually eroded. Furthermore, we plot the empirical **BP lower bound**, achieved by decoding with a 5-iterations BP over all  $\kappa = n \log_2(n+1)$  permutations; and selecting the output word by the *argmax* criterion mentioned above.

In Fig. 4 the reported results are for BCH(63,45). We observed

<sup>1</sup>The base of the logarithm is  $e$ .

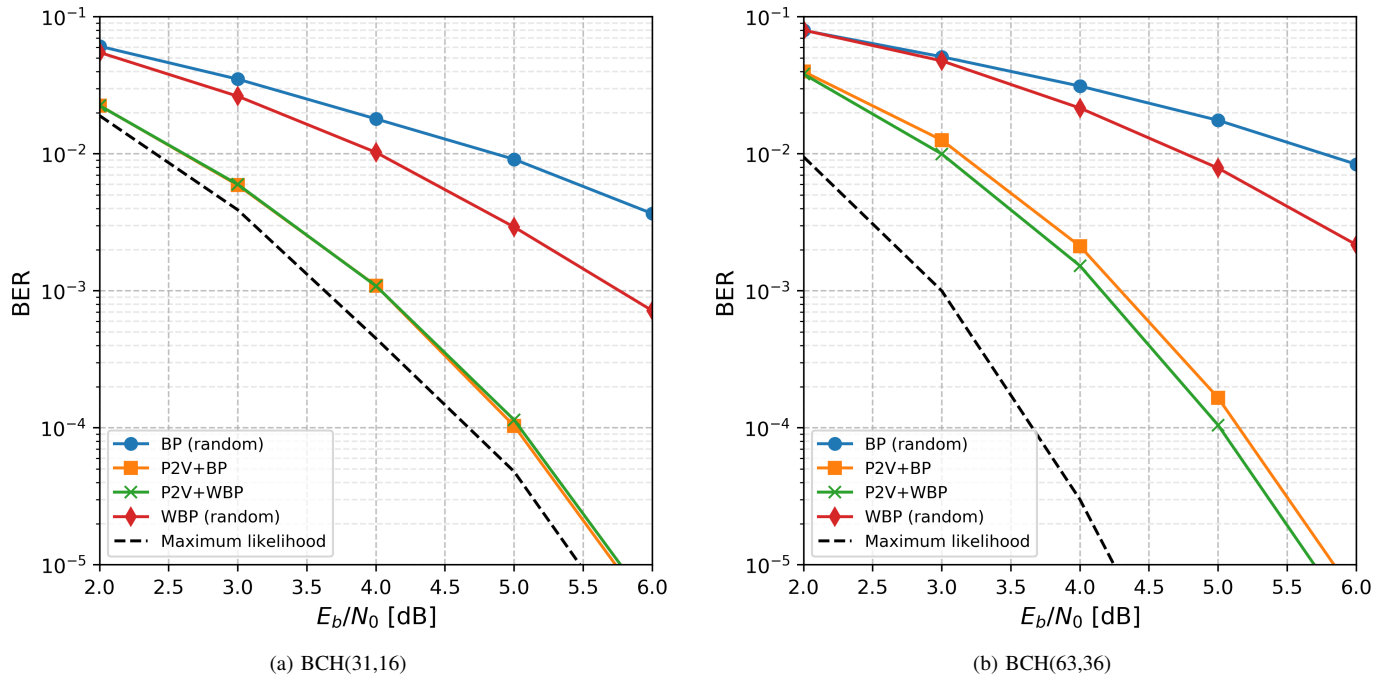


Fig. 3: BER vs. SNR for `perm2vec` and random permutation selection. Both BP and WBP are considered.

TABLE II: A comparison of the BER negative decimal logarithm for three SNR values [dB]. Higher is better. We bold the best results and underlined the second ones.

BCH ( $n,k$ )	BP (random)			WBP (random)			P2V + BP			P2V + WBP		
	2	4	6	2	4	6	2	4	6	2	4	6
	— TOP 1 —											
(31,16)	1.21	1.74	2.44	1.26	1.99	3.14	<b>1.65</b>	<b>2.96</b>	<b>5.37</b>	<u>1.65</u>	<u>2.96</u>	<u>5.31</u>
(63,36)	1.10	1.51	2.08	1.10	1.67	2.66	<u>1.40</u>	<u>2.67</u>	<u>5.23</u>	<b>1.42</b>	<b>2.82</b>	<b>5.44</b>
(63,45)	1.26	1.90	2.81	1.25	2.08	3.67	<u>1.40</u>	<u>2.58</u>	<u>5.01</u>	<b>1.42</b>	<b>2.73</b>	<b>5.35</b>
(127,64)	0.99	1.30	1.74	0.99	1.32	2.11	<u>1.01</u>	<u>1.94</u>	<u>4.04</u>	<b>1.01</b>	<b>1.98</b>	<b>4.14</b>
	— TOP 5 —											
(31,16)	1.49	2.55	4.17	1.43	2.52	4.12	<b>1.72</b>	<b>3.12</b>	<b>5.59</b>	<u>1.69</u>	<u>3.09</u>	<u>5.57</u>
(63,36)	1.18	2.04	3.36	1.18	2.12	3.84	<u>1.47</u>	<u>2.96</u>	<u>5.78</u>	<b>1.49</b>	<b>3.11</b>	<b>6.07</b>
(63,45)	1.33	2.41	4.26	1.30	2.48	4.91	<u>1.45</u>	<u>2.85</u>	<u>5.65</u>	<b>1.45</b>	<b>2.98</b>	<b>5.92</b>
(127,64)	0.99	1.49	2.66	0.99	1.51	2.88	<u>1.01</u>	<u>2.10</u>	<u>4.62</u>	<b>1.02</b>	<b>2.11</b>	<b>4.70</b>

an improvement of 0.4 dB between  $\kappa = 1$  and  $\kappa = 5$  and only 0.2 dB between  $\kappa = 5$  and  $\kappa = 10$ . Furthermore, the gap between  $\kappa = 10$  and the BP lower bound is small (0.4 dB).

*c) Embedding Size Evaluation:* In Fig. 5 we present the performance of our method using two embedding sizes. We compare our **base** model, that uses embedding size  $d_q = 80$  against the **small** model, that uses embedding size  $d_q = 20$  (note that  $d_q = d_w$ ). We further state that changing the embedding size affects also the number of parameters in  $g$ , as in Eq. (5).

Using a smaller embedding size causes a slight degradation to performance, yet still dramatically improving the random BP baseline. For the shorter BCH(63,36), the gap is 0.5 dB and for the longer BCH(127,64) the gap is 0.2 dB.

## V. RELATED WORK

Permutation decoding (PD) has earned new attention [32]–[34] due to accomplished gains presented for 5G-standard approved polar codes. [32] suggests a novel PD method for these codes. Yet, the main novelty lies in the proposed stopping criteria for the list decoder, while the permutations are chosen in a random fashion. The authors of [33] present an algorithm to form a permutation set, computed by fixing several first layers of the underlying structure of the polar decoder, and solely permuting the last layers. The original graph is included in this set as a default, with additional permutations added in the process of a limited-space search. Lastly, we refer to [34] which proposes a successive permutations scheme that finds suitable permutations as decoding progresses. Again, due to

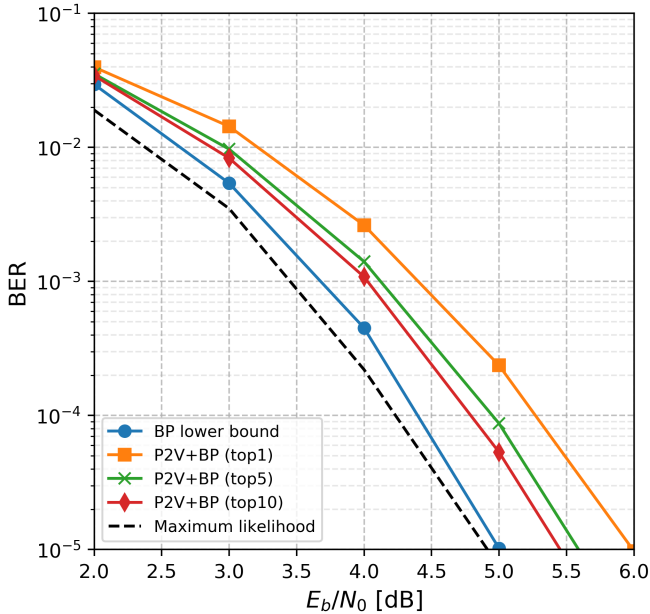


Fig. 4: BER vs. SNR for top- $\kappa$  permutation selection, with code BCH(63,45).

the exploding search space, they only consider the cyclic shifts of each layer. This limited-search has first appeared in [35].

Most PD methods, as the ones mentioned above, suggest several valuable additions. We, on the other hand, see the choice of permutation as the most integral part of PD, suggesting a pre-decoding module to choose the most fitting one. As such, we point out that direct comparison between the PD model-based works mentioned and ours cannot be done.

Regarding model-free approaches, we refer to the particular work [36] since it integrates permutation groups into a model-free approach. In the mentioned paper, the decoding network accepts the syndrome of the hard decisions as part of the input. This way, domain knowledge is incorporated to the model-free approach. We introduce domain knowledge by training the permutation transformer on the parity-check matrix *and* accepting the permuted syndrome. Furthermore, each word is chosen a fitting permutation such that the sum of LLRs in the positions of the information-bits is maximized. Observe that this approach only benefits model-free decoders. Overall, comparison to our work can't be made in this case as well.

## VI. CONCLUSION

We presented a promising new framework for the application of neural Transformer network to improve decoding of linear error correction codes. For every code and received noisy word, the proposed model fits a permutation out of the code's PG set which introduces improved decoding capabilities. Our method pre-computes the permutations' representations thus allowing fast and accurate permutation selection at the inference phase. Furthermore, our method is independent of the code length and therefore is considered scalable. We demonstrate the effectiveness of `perm2vec` by showing significant BER performance improvements, compared to the baseline decoding

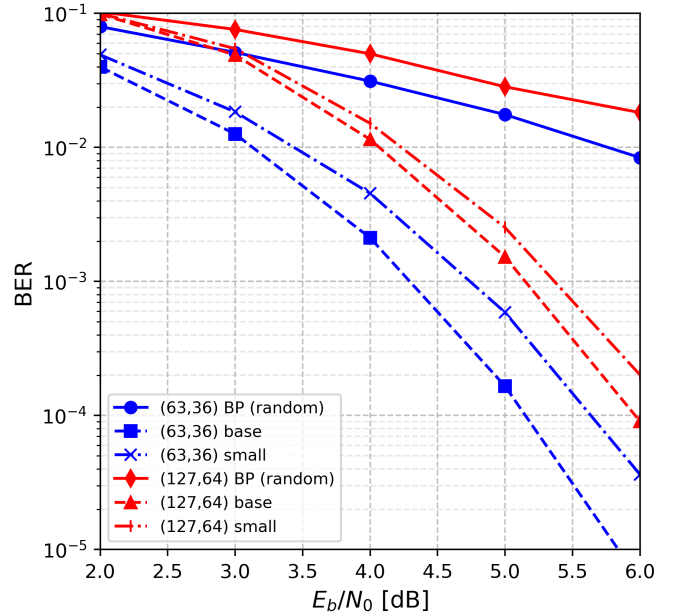


Fig. 5: Performance comparison for different embedding size.

algorithms for various code lengths. Future research should extend our method to polar codes, replacing the embedded Tanner graph variable nodes to embedded factor graph variable nodes. Another possible research direction is to train both `perm2vec` and WBP jointly in an end-to-end manner, or considering an iterative training solution that alternates between training the graph permutation selection model and the WBP algorithm (or any other trainable decoder).

## REFERENCES

- [1] C. E. Shannon, "A mathematical theory of communication," *Bell system technical journal*, vol. 27, no. 3, 1948.
- [2] J. Pearl, *Probabilistic reasoning in intelligent systems: networks of plausible inference*. Elsevier, 2014.
- [3] J. Macwilliams, "Permutation decoding of systematic codes," *The Bell System Technical Journal*, vol. 43, no. 1, 1964.
- [4] I. Dimnik and Y. Be'ery, "Improved random redundant iterative hdpc decoding," *IEEE Transactions on Communications*, 2009.
- [5] A. Elkelesh, M. Ebada, S. Cammerer, and S. ten Brink, "Belief propagation list decoding of polar codes," *IEEE Communications Letters*, 2018.
- [6] O. Simeone, "A very brief introduction to machine learning with applications to communication systems," *IEEE Transactions on Cognitive Communications and Networking*, 2018.
- [7] A. Zappone, M. Di Renzo, and M. Debbah, "Wireless networks design in the era of deep learning: Model-based, ai-based, or both?" *arXiv preprint arXiv:1902.02647*, 2019.
- [8] M. I. Belghazi, A. Baratin, S. Rajeswar, S. Ozair, Y. Bengio, A. Courville, and R. D. Hjelm, "Mine: mutual information neural estimation," *arXiv preprint arXiv:1801.04062*, 2018.
- [9] A. Caciularu and D. Burshtein, "Blind channel equalization using variational autoencoders," in *International Conference on Communications Workshops (ICC Workshops)*, 2018.
- [10] A. Caciularu and D. Burshtein, "Unsupervised linear and nonlinear channel equalization and decoding using variational autoencoders," *arXiv preprint arXiv:1905.08795*, 2019.
- [11] X. Lin, I. Sur, S. A. Nastase, A. Divakaran, U. Hasson, and M. R. Amer, "Data-efficient mutual information neural estimator," *arXiv preprint arXiv:1905.03319*, 2019.
- [12] I. Beery, N. Raviv, T. Raviv, and Y. Beery, "Active deep decoding of linear codes," *IEEE Transactions on Communications*, 2019.

- [13] O. Simeone, S. Park, and J. Kang, "From learning to meta-learning: Reduced training overhead and complexity for communication systems," *arXiv preprint arXiv:2001.01227*, 2020.
- [14] T. Gruber, S. Cammerer, J. Hoydis, and S. ten Brink, "On deep learning-based channel decoding," in *51st Annual Conference on Information Sciences and Systems (CISS)*, 2017.
- [15] H. Kim, Y. Jiang, R. Rana, S. Kannan, S. Oh, and P. Viswanath, "Communication algorithms via deep learning," *arXiv preprint arXiv:1805.09317*, 2018.
- [16] E. Nachmani, Y. Be'ery, and D. Burshtein, "Learning to decode linear codes using deep learning," in *Annual Allerton Conference on Communication, Control, and Computing (Allerton)*, 2016.
- [17] E. Nachmani, E. Marciano, D. Burshtein, and Y. Be'ery, "RNN decoding of linear block codes," *arXiv preprint arXiv:1702.07560*, 2017.
- [18] E. Nachmani, E. Marciano, L. Lugosch, W. J. Gross, D. Burshtein, and Y. Beery, "Deep learning methods for improved decoding of linear codes," *IEEE Journal of Selected Topics in Signal Processing*, 2018.
- [19] T. Raviv, N. Raviv, and Y. Be'ery, "Data-driven ensembles for deep and hard-decision hybrid decoding," *arXiv preprint arXiv:2001.06247*, 2020.
- [20] A. Vaswani, N. Shazeer, N. Parmar, J. Uszkoreit, L. Jones, A. N. Gomez, L. u. Kaiser, and I. Polosukhin, "Attention is all you need," in *Advances in Neural Information Processing Systems 30*, 2017.
- [21] T. Richardson and R. Urbanke, *Modern coding theory*. Cambridge university press, 2008.
- [22] A. Dehghan and A. H. Banihashemi, "On the tanner graph cycle distribution of random LDPC, random protograph-based LDPC, and random quasi-cyclic LDPC code ensembles," *IEEE Transactions on Information Theory*, 2018.
- [23] K. Guenda, "The permutation groups and the equivalence of cyclic and quasi-cyclic codes," *arXiv preprint arXiv:1002.2456*, 2010.
- [24] F. J. MacWilliams and N. J. A. Sloane, *The theory of error-correcting codes*. Elsevier, 1977, vol. 16.
- [25] A. Grover and J. Leskovec, "node2vec: Scalable feature learning for networks," in *22nd ACM SIGKDD International Conference on Knowledge Discovery and Data Mining*, 2016.
- [26] D. Bahdanau, K. Cho, and Y. Bengio, "Neural machine translation by jointly learning to align and translate," in *3rd International Conference on Learning Representations, ICLR*, 2015.
- [27] J. Devlin, M.-W. Chang, K. Lee, and K. Toutanova, "BERT: Pre-training of deep bidirectional transformers for language understanding," in *Conference of the North American Chapter of the Association for Computational Linguistics: Human Language Technologies*, 2019.
- [28] Y. Liu, M. Ott, N. Goyal, J. Du, M. Joshi, D. Chen, O. Levy, M. Lewis, L. Zettlemoyer, and V. Stoyanov, "Roberta: A robustly optimized bert pretraining approach," *arXiv preprint arXiv:1907.11692*, 2019.
- [29] Z. Yang, Z. Dai, Y. Yang, J. Carbonell, R. Salakhutdinov, and Q. V. Le, "Xlnet: Generalized autoregressive pretraining for language understanding," *arXiv preprint arXiv:1906.08237*, 2019.
- [30] M. Joshi, O. Levy, L. Zettlemoyer, and D. Weld, "BERT for coreference resolution: Baselines and analysis," in *Conference on Empirical Methods in Natural Language Processing and the 9th International Joint Conference on Natural Language Processing (EMNLP-IJCNLP)*, 2019.
- [31] A. Wang, A. Singh, J. Michael, F. Hill, O. Levy, and S. Bowman, "GLUE: A multi-task benchmark and analysis platform for natural language understanding," in *EMNLP Workshop BlackboxNLP: Analyzing and Interpreting Neural Networks for NLP*, 2018.
- [32] M. Kamenev, Y. Kameneva, O. Kurmaev, and A. Maevskiy, "A new permutation decoding method for reed-muller codes," *arXiv preprint arXiv:1901.04433*, 2019.
- [33] N. Doan, S. A. Hashemi, M. Mondelli, and W. J. Gross, "On the decoding of polar codes on permuted factor graphs," in *Global Communications Conference (GLOBECOM)*, 2018.
- [34] S. A. Hashemi, N. Doan, M. Mondelli, and W. J. Gross, "Decoding reed-muller and polar codes by successive factor graph permutations," in *10th International Symposium on Turbo Codes & Iterative Information Processing (ISTC)*, 2018.
- [35] S. B. Korada, "Polar codes for channel and source coding," EPFL, Tech. Rep. 4461, 2009.
- [36] A. Bennatan, Y. Choukroun, and P. Kisilev, "Deep learning for decoding of linear codes-a syndrome-based approach," in *International Symposium on Information Theory (ISIT)*, 2018.